An Iterative Information-Reduced Quadriphase-Shift-Keyed Carrier Synchronization Scheme Using Decision Feedback for Low Signal-to-Noise Ratio Applications

M. Simon[1] and A. Tkacenko[1]

In a previous publication [1], an iterative closed-loop carrier synchronization scheme for binary phase-shift keyed (BPSK) modulation was proposed that was based on feeding back data decisions to the input of the loop, the purpose being to remove the modulation prior to carrier synchronization as opposed to the more conventional decision-feedback schemes that incorporate such feedback inside the loop. The idea there was that, with sufficient independence between the received data and the decisions on it that are fed back (as would occur in an error-correction coding environment with sufficient decoding delay), a "pure" tone in the presence of noise would ultimately be produced (after sufficient iteration and low enough error probability) and thus could be tracked without any squaring loss. This article demonstrates that, with some modification, the same idea of iterative information reduction through decision feedback can be applied to quadrature phase-shift keyed (QPSK) modulation, something that was mentioned in the previous publication but never pursued.

I. Introduction

In recent years there has been an ever-increasing interest in and application of highly power efficient error-correction codes such as turbo codes and low-density parity check (LDPC) codes to NASA-sponsored programs. These codes, which approach the Shannon channel capacity of the system, operate at very low symbol signal-to-noise ratios (SNRs), thus necessitating the need for synchronization (sync) (e.g., carrier, symbol, etc.) schemes that likewise operate efficiently at these SNRs. To begin to address this issue, several years ago the notion of iterative information-reduced carrier synchronization for coded binary phase-shift-keyed (BPSK) modulation was introduced [1]. The idea behind this notion was to overcome the penalty in noisy reference loss attributed to the large squaring loss at low SNRs that is characteristic of the traditional types of BPSK carrier synchronization loops, e.g., the Costas or in-phase–quadrature phase (I-Q) loop, by removing the modulation from the received signal *prior* to demodulation, thus

allowing instead the use of a phase-locked loop (PLL). The process by which the modulation was removed (information reduced) was envisioned as an iterative one wherein hard decisions on the data produced by the data detector/decoder would be fed back and applied to (multiplied by) the received signal, thus improving the carrier synchronization, which in turn would improve the data detector performance, hence the data decisions fed back on the next iteration, and so on. At the same time, the loop would be adapting its parameters (i.e., the loop nonlinearity in the in-phase arm) to match the current fidelity of the data decision process, all the while shifting its configuration from a Costas-type loop toward a PLL in the limit of perfect detection. Several publications based on this notion appeared in the literature and included everything from the basic idea and accompanying analysis/performance evaluations [1] to successful application and implementation for specific error-correcting codes [2,3].

With the continued shift toward increased bandwidth efficiency using modulations such as quadriphase-shift keying (QPSK), it became apparent, and was alluded to in the conclusions of [1], that the same ideas could be applied in this case, where the problem of nonlinear (e.g., quadrupling) loss (analogous to squaring loss for the BPSK case) at low SNRs becomes exacerbated. However, the manner in which the fed-back decisions are used for information removal is somewhat different since in addition to producing the desired (information-reduced) signal on, say, the I (or Q) channel, one now also generates an undesired (cross-talk) signal on the Q (or I) channel. A positive solution to this problem is proposed in this article and will be referred to as *iterative QPSK information-reduced carrier sync*. As in the BPSK case, the scheme is motivated by maximum a posteriori (MAP) estimation of carrier phase considerations. Section II presents the derivation of the closed-loop architecture. Section III derives the tracking performance of the loop in terms of its mean-square phase error when operating in the linear (high loop SNR) region, as is typical. Section IV presents the asymptotic behavior of this performance in the limit of low SNR and compares it with that of the conventional QPSK tracking loop that does not make use of decision feedback for information reduction. Section V presents the numerical illustration of the loop tracking performance and compares it with that of the conventional loop mentioned above. Section VI explores the sensitivity of the scheme to mismatch between the actual value of symbol-error probability of the I and Q data decoders and the estimate of it used in the loop implementation. Finally, Section VII documents our conclusions.

II. MAP Estimation of Carrier Phase for QPSK with Unbalanced Data

Consider the transmission of a QPSK signal over an additive white Gaussian noise (AWGN) channel whereupon the received signal has the form $x(t;\theta) = s(t;\theta) + n(t)$, where

$$s(t;\theta) = \sqrt{S}m_1(t)\sin(\omega_c t + \theta) + \sqrt{S}m_2(t)\cos(\omega_c t + \theta) \tag{1}$$

and the additive noise has the narrowband expansion

$$n(t) = \sqrt{2}\big[n_c(t)\cos(\omega_c t + \theta) - n_s(t)\sin(\omega_c t + \theta)\big] \tag{2}$$

In Eq. (1), S denotes the received signal power, θ is random (assumed to be uniformly distributed and time independent) carrier phase, and $m_1(t)$ and $m_2(t)$ are the I and Q modulations, which are described by binary pulse trains as

$$m_1(t) = \sum_{k=-\infty}^{\infty} a_k p(t - kT)$$

$$\text{(3)}$$

$$m_2(t) = \sum_{k=-\infty}^{\infty} b_k p(t - kT)$$

where $p(t)$ is a unit power rectangular pulse of duration T and $\{a_k\}, \{b_k\}$ are each equiprobable independent, identically distributed (i.i.d.) binary (± 1) sequences that are also independent of each other. The noise process in Eq. (2) is modeled in terms of a pair of independent, low-pass Gaussian processes, $n_c(t), n_s(t)$, each with single-sided power spectral density (PSD) N_0 W/Hz and bandwidth $B_H < \omega_c/2\pi$.

With reference to the ad hoc structure illustrated in Fig. 1, the received signal-plus-noise $x(t; \theta)$ is delayed by an amount Δ (to match the decoding delay of the I-channel data) and multiplied by the data estimator waveform

$$\hat{m}_1(t - \Delta) = \sum_{k=-\infty}^{\infty} \hat{a}_k p(t - kT - \Delta) \tag{4}$$

to form the signal $y_1(t) = x(t - \Delta; \theta)\,\hat{m}_1(t - \Delta)$. Similarly, the received signal plus noise $x(t; \theta)$ is shifted by $-\pi/2$ rad, delayed by an amount Δ (to match the decoding delay of the Q-channel data assumed to be the same as that of the I-channel decoding delay) and multiplied by the data estimator waveform

$$\hat{m}_2(t - \Delta) = \sum_{k=-\infty}^{\infty} \hat{b}_k p(t - kT - \Delta) \tag{5}$$

to form the signal $y_2(t) = x(t - \Delta; \theta - \pi/2)\,\hat{m}_2(t - \Delta)$. Assuming, as in the previous publications on the subject, that the sequences of estimates $\{\hat{a}_k\}, \{\hat{b}_k\}$ are each i.i.d. sequences and have the probability statistics (based on error probability associated with the particular coding/decoding model employed)

$$\Pr\{\hat{a}_k \neq a_k\} = p_1, \quad \Pr\{\hat{a}_k = a_k\} = 1 - p_1$$

$$\text{(6)}$$

$$\Pr\{\hat{b}_k \neq b_k\} = p_2, \quad \Pr\{\hat{b}_k = b_k\} = 1 - p_2$$

then the results of the above-mentioned products become

$$y_1(t) = \sqrt{S}m_1(t - \Delta)\,\hat{m}_1(t - \Delta)\sin(\omega_c t + \theta) + \sqrt{S}m_2(t - \Delta)\,\hat{m}_1(t - \Delta)\cos(\omega_c t + \theta) + n_1(t)$$

$$= \sqrt{S}e_{11}(t)\sin(\omega_c t + \theta) + \sqrt{S}e_{21}(t)\cos(\omega_c t + \theta) + n_1(t)$$

$$\text{(7)}$$

$$y_2(t) = -\sqrt{S}m_1(t - \Delta)\,\hat{m}_2(t - \Delta)\cos(\omega_c t + \theta) + \sqrt{S}m_2(t - \Delta)\,\hat{m}_2(t - \Delta)\sin(\omega_c t + \theta) + n_2(t)$$

$$= -\sqrt{S}e_{12}(t)\cos(\omega_c t + \theta) + \sqrt{S}e_{22}(t)\sin(\omega_c t + \theta) + n_2(t)$$

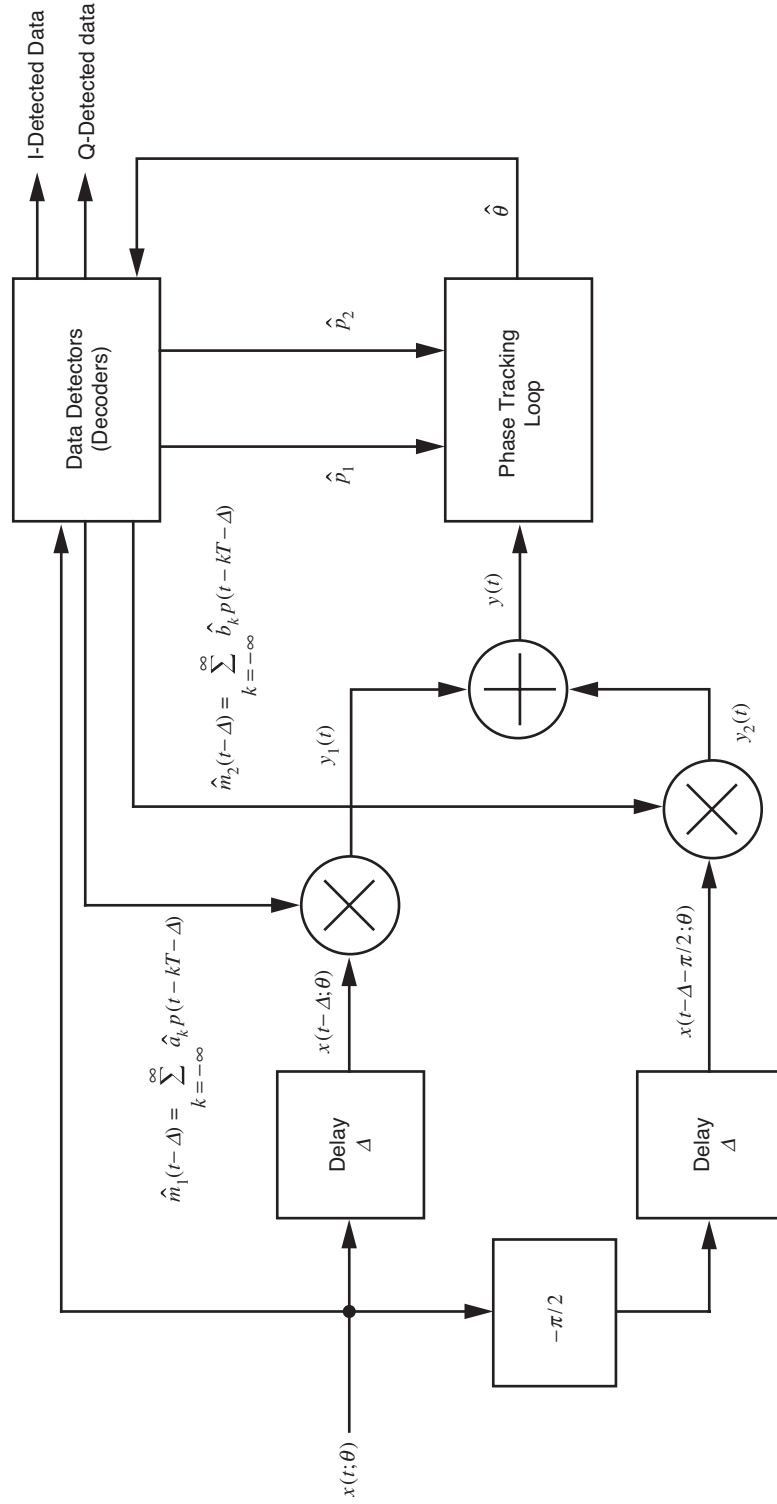**Fig. 1. QPSK receiver with information-reduced carrier phase estimation.**

I-Detected Data

Q-Detected data

Data Detectors (Decoders)

Phase Tracking Loop

$\hat{\theta}$

$\hat{p}_2$

$\hat{p}_1$

$\hat{m}_2(t-\Delta) = \sum\limits_{k=-\infty}^{\infty} \hat{b}_k\, p(t-kT-\Delta)$

$y(t)$

$y_1(t)$

$y_2(t)$

$\hat{m}_1(t-\Delta) = \sum\limits_{k=-\infty}^{\infty} \hat{a}_k\, p(t-kT-\Delta)$

$x(t-\Delta;\theta)$

$x(t-\Delta-\pi/2;\theta)$

Delay Δ

Delay Δ

$-\pi/2$

$x(t;\theta)$

where we have arbitrarily absorbed the additional carrier phase, $\omega_c \Delta$, due to the decoding delay in the unknown carrier phase θ. The baseband modulation waveforms $e_{11}(t), e_{22}(t), e_{12}(t), e_{21}(t)$ that reflect the errors in the detection of the I and Q input data sequences are modeled as[2]

$$e_{11}(t) = \sum_{k=-\infty}^{\infty} e_{11k} p(t - kT), \quad e_{22}(t) = \sum_{k=-\infty}^{\infty} e_{22k} p(t - kT)$$

$$e_{12}(t) = \sum_{k=-\infty}^{\infty} e_{12k} p(t - kT), \quad e_{21}(t) = \sum_{k=-\infty}^{\infty} e_{21k} p(t - kT)$$

(8)

where

$$e_{11k} = a_k \hat{a}_k, \quad e_{22k} = b_k \hat{b}_k, \quad e_{12k} = a_k \hat{b}_k, \quad e_{21k} = \hat{a}_k b_k \tag{9}$$

are binary (± 1) sequences with probability statistics

$$\Pr\{e_{iik} = -1\} = p_i, \quad \Pr\{e_{iik} = 1\} = 1 - p_i, \quad i = 1, 2$$

(10)

$$\Pr\{e_{12k} = -1\} = \Pr\{e_{12k} = 1\} = \Pr\{e_{21k} = -1\} = \Pr\{e_{21k} = 1\} = \frac{1}{2}$$

The additive noises in Eq. (7), namely, $n_1(t) = \hat{m}_1(t - \Delta)\sqrt{2}\big[n_c(t)\cos(\omega_c t + \theta) - n_s(t)\sin(\omega_c t + \theta)\big]$ and $n_2(t) = \hat{m}_2(t - \Delta)\sqrt{2}\big[n_c(t)\sin(\omega_c t + \theta) + n_s(t)\cos(\omega_c t + \theta)\big]$ are AWGN in each T-second interval with statistics identical to $n(t)$ and are independent of the data. Note that to the extent that $\hat{m}_1(t - \Delta)$ and $\hat{m}_2(t - \Delta)$ are independent, $n_1(t)$ and $n_2(t)$ are independent.

In an effort to eliminate the quadrature-modulated carrier (cross-talk) term, we next form the sum of $y_1(t)$ and $y_2(t)$, resulting in

$$y(t) = y_1(t) + y_2(t)$$

$$= \sqrt{S}\big[e_1(t) + e_2(t)\big]\sin(\omega_c t + \theta) + \sqrt{S}\big[e_{21}(t) - e_{12}(t)\big]\cos(\omega_c t + \theta) + n_1(t) + n_2(t) \tag{11}$$

$$= \sqrt{S}E_d(t)\sin(\omega_c t + \theta) + \sqrt{S}E_u(t)\cos(\omega_c t + \theta) + n_1(t) + n_2(t)$$

where the "d" subscript denotes the *desired* signal to be tracked and the "u" subscript denotes the residual *undesired* cross-talk signal; $E_d(t)$ and $E_u(t)$ are ternary waveforms that can be expressed as

$$E_d(t) = \sum_{k=-\infty}^{\infty} E_{dk} p(t - kT)$$

(12)

$$E_u(t) = \sum_{k=-\infty}^{\infty} E_{uk} p(t - kT)$$

---

[2] Without loss in generality, for simplicity of notation we herein ignore the decoding delay.

where $\left\{E_{dk} = a_k\hat{a}_k + b_k\hat{b}_k\right\}$ and $\left\{E_{uk} = \hat{a}_k b_k - a_k\hat{b}_k\right\}$ are ternary $(0, \pm2)$ i.i.d. sequences with probability distributions as follows:

$$P\left\{E_{dk}\right\} = \begin{cases} (1 - p_1)(1 - p_2), & E_{dk} = 2 \\ p_1 p_2, & E_{dk} = -2 \\ p_1(1 - p_2) + p_2(1 - p_1), & E_{dk} = 0 \end{cases} \tag{13}$$

and

$$P\left\{E_{uk}\right\} = \begin{cases} \frac{1}{2}p_1(1 - p_2) + \frac{1}{2}p_2(1 - p_1), & E_{uk} = \pm2 \\ 1 - p_1(1 - p_2) - p_2(1 - p_1), & E_{uk} = 0 \end{cases} \tag{14}$$

For equal decoding probabilities, i.e., $p_1 = p_2 = p$, Eqs. (13) and (14) simplify to

$$P\left\{E_{dk}\right\} = \begin{cases} (1 - p)^2, & E_{dk} = 2 \\ p^2, & E_{dk} = -2 \\ 2p(1 - p), & E_{dk} = 0 \end{cases} \tag{15}$$

and

$$P\left\{E_{uk}\right\} = \begin{cases} p(1 - p), & E_{uk} = \pm2 \\ 1 - 2p(1 - p), & E_{uk} = 0 \end{cases} \tag{16}$$

For $p = 1/2$, they have identical first-order statistics given by

$$P\left\{E_{dk}\right\} = P\left\{E_{uk}\right\} \triangleq P\left\{E_k\right\} = \begin{cases} \dfrac{1}{4}, & E_k = \pm2 \\ \dfrac{1}{2}, & E_k = 0 \end{cases} \tag{17}$$

Note that the sequences $\left\{E_{dk}\right\}$ and $\left\{E_{uk}\right\}$ are uncorrelated for all values of p but *are not independent.* Their joint statistics are given by

$$P\left\{E_{dk}, E_{uk}\right\} = \begin{cases} (1 - p)^2, & E_{dk} = 2, E_{uk} = 0 \\ p^2, & E_{dk} = -2, E_{uk} = 0 \\ p(1 - p), & E_{dk} = 0, E_{uk} = \pm2 \\ 0, & \text{otherwise} \end{cases} \tag{18}$$

Thus, when $p = 1/2$ (i.e., in the very early stages of iteration when the loop begins to operate without reliable data decisions), the signal component of the input to the loop as characterized in Eq. (11) appears as an I-Q modulation with identically distributed (but not independent) ternary modulations on each

arm. On the other hand, when p becomes small (the desirable case for reliable data detection), then in the limit as $p \to 0$, the signal component of the loop input becomes a pure (unmodulated) sinusoidal tone, which can be tracked by a PLL that exhibits the least degradation in performance.

Returning now to the determination of the MAP estimate of phase, the combined signal plus noise in Eq. (11) is observed for K data intervals, i.e., over the interval $0 \le t \le KT$. Based on this observation and knowledge of $S, p(t)$ and ω_c, the MAP estimate of phase is that value $\hat{\theta}_{\mathrm{MAP}}$ that maximizes the conditional probability density function $p(\theta|y(t))$ or, equivalently, the likelihood function $p(y(t)|\theta)$. As in previous analyses for equiprobable data statistics, the likelihood function (LF) conditioned on the data sequences $\{E_{dk}\}$ and $\{E_{uk}\}$ in the K-symbol observation is given by (disregarding a proportionality constant)[3]

$$p\big(y(t)|\theta, \{E_{dk}\}, \{E_{uk}\}\big) = \prod_{k=0}^{K-1} \exp\big(E_{dk}y_{sk}(\theta)\big) \exp\big(E_{uk}y_{ck}(\theta)\big) \exp\left[-\frac{R_d}{4}\big(E_{dk}^2 + E_{uk}^2\big)\right] \qquad (19)$$

where $R_d \triangleq ST/N_0$ denotes the symbol signal-to-noise ratio (SNR) and

$$y_{sk}(\theta) \triangleq \frac{\sqrt{S}}{N_0} \int_{kT}^{(k+1)T} y(t) \sin(\omega_c t + \theta)\, dt$$

$$\qquad (20)$$

$$y_{ck}(\theta) \triangleq \frac{\sqrt{S}}{N_0} \int_{kT}^{(k+1)T} y(t) \cos(\omega_c t + \theta)\, dt$$

Jointly averaging Eq. (19) over the statistics of the data sequences $\{E_{dk}\}$ and $\{E_{uk}\}$ as given in Eq. (18) results in the unconditional LF[4]

$$\Lambda(\theta) = p\big(y(t)|\theta\big) = \prod_{k=0}^{K-1} \exp(-R_d)\left[(1-p)^2 \exp\big(2y_{sk}(\theta)\big) + p^2 \exp\big(-2y_{sk}(\theta)\big)\right.$$

$$\left. + 2p(1-p)\cosh\big(2y_{ck}(\theta)\big)\right] \qquad (21)$$

Taking the natural logarithm of Eq. (21) gives the log-likelihood function (LLF)

$$\ln \Lambda(\theta) = -KR_d + \sum_{k=0}^{K-1} \ln\left[(1-p)^2 \exp\big(2y_{sk}(\theta)\big) + p^2 \exp\big(-2y_{sk}(\theta)\big)\right.$$

$$\left. + 2p(1-p)\cosh\big(2y_{ck}(\theta)\big)\right] \qquad (22)$$

The MAP phase estimate $\hat{\theta}_{MAP}$ is then the solution to

---

[3] Note that, because of the ternary nature of the effective I and Q data sequences $\{E_{dk}\}$ and $\{E_{uk}\}$, we temporarily retain the energy term in Eq. (19), $\exp\left[-(R_d/4)\big(E_{dk}^2 + E_{uk}^2\big)\right]$, since, unlike the binary data case, it is possible that it is not independent of the data sequence. Shortly we shall show that indeed because of the dependence of E_{dk} and E_{uk} on each other, the term $E_{dk}^2 + E_{uk}^2$ only takes on the value 4, and thus this term may be dropped in the likelihood function.

[4] For simplicity, we pursue the equal decoding probability case.

$$\hat{\theta}_{\mathrm{MAP}} = \max_{\theta}{}^{-1} \ln \Lambda(\theta) \qquad (23)$$

Note that as the decoding error probability iteratively improves and eventually becomes vanishingly small, in the limit of $p \to 0$, Eq. (22) simplifies to (ignoring the constant additive term)

$$\ln \Lambda(\theta) = 2 \sum_{k=0}^{K-1} y_{sk}(\theta) \qquad (24)$$

which is the appropriate result for the LLF in the case of an unmodulated carrier.

Since by definition $\hat{\theta}_{\mathrm{MAP}}$ is the value of θ that maximizes the LLF, an equivalent statement is that $\hat{\theta}_{\mathrm{MAP}}$ is the value of θ at which the derivative of the LLF has zero value (and the second derivative is negative). For estimates $\hat{\theta}$ of θ in the neighborhood of $\hat{\theta}_{\mathrm{MAP}}$, the derivative of the LLF will be positive or negative in accordance with the sign of $\theta - \hat{\theta}_{\mathrm{MAP}}$; thus, this derivative can be used as an error signal in a closed-loop synchronizer to steer the loop in the direction of a locked condition corresponding to $\theta = \hat{\theta}_{\mathrm{MAP}}$. Taking the derivative of Eq. (22) with respect to θ gives

$$\frac{d}{d\theta} \ln \Lambda(\theta) = 2 \sum_{k=0}^{K-1} \frac{(1-p)^2 \exp\left(2y_{sk}(\theta)\right) - p^2 \exp\left(-2y_{sk}(\theta)\right)}{(1-p)^2 \exp\left(2y_{sk}(\theta)\right) + p^2 \exp\left(-2y_{sk}(\theta)\right) + 2p(1-p)\cosh\left(2y_{ck}(\theta)\right)} y_{ck}(\theta)$$

$$- 2 \sum_{k=0}^{K-1} \frac{2p(1-p)\sinh\left(2y_{ck}(\theta)\right)}{(1-p)^2 \exp\left(2y_{sk}(\theta)\right) + p^2 \exp\left(-2y_{sk}(\theta)\right) + 2p(1-p)\cosh\left(2y_{ck}(\theta)\right)} y_{sk}(\theta) \quad (25)$$

which suggests a cross-over type closed loop with cross-coupled nonlinearities in its I and Q arms, where by "cross-coupled" is meant the fact that each one acts on *both* the I and Q amplified matched filter outputs. In particular, in accordance with Eq. (25), defining the two-dimensional nonlinearities

$$f_1(u, v) \triangleq \frac{2\left[(1-p)^2 \exp(2u) - p^2 \exp(-2u)\right]}{(1-p)^2 \exp(2u) + p^2 \exp(-2u) + 2p(1-p)\cosh(2v)} \qquad (26)$$

and

$$f_2(u, v) \triangleq \frac{4p(1-p)\sinh(2v)}{(1-p)^2 \exp(2u) + p^2 \exp(-2u) + 2p(1-p)\cosh(2v)} \qquad (27)$$

then the closed-loop QPSK carrier synchronizer motivated by the MAP estimation procedure is as illustrated in Fig. 2, where the value of p to be used in forming the nonlinearities $f_1(u, v)$ and $f_2(u, v)$ is derived from an estimate $\hat{p}$ provided by the data detectors and is iteratively updated. We herein refer to this loop as the *MAP estimation loop for QPSK with unbalanced data*. Note that, for $p \to 0$, $f_1(u, v) \to 2$ and $f_2(u, v) = 0$, in which case Eq. (25) simplifies to

$$\frac{d}{d\theta} \ln \Lambda(\theta) = 2 \sum_{k=0}^{K-1} y_{ck}(\theta) \qquad (28)$$
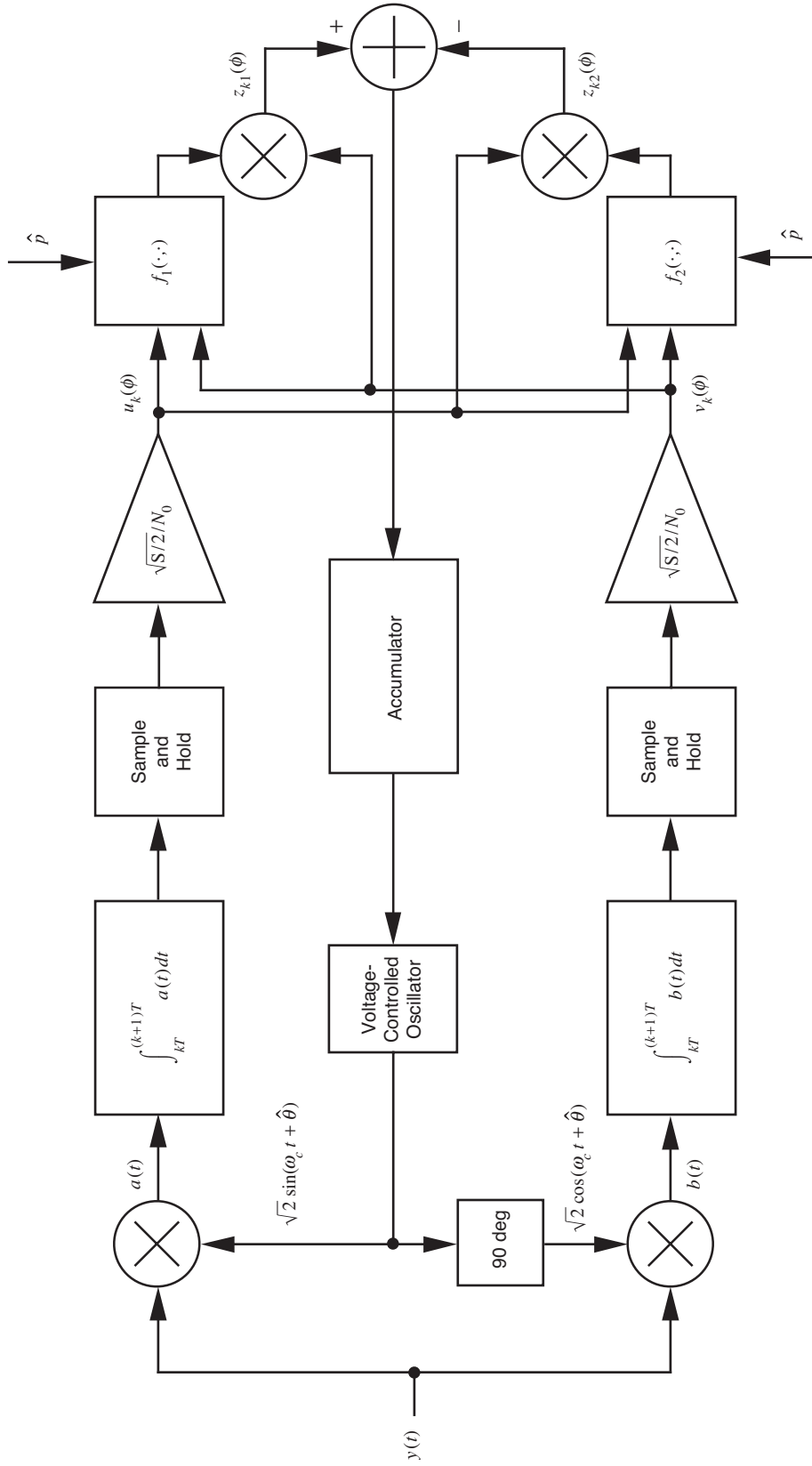
Fig. 2. Information-reduced carrier synchronization loop.

9

which also can be immediately determined from Eq. (24). In principle, this is the same result that would occur for BPSK and suggests that, in the limit of vanishingly small decoding error probability, the closed loop behaves similarly to a phase-locked loop (PLL) since no quadrature arm is required in its implementation.

Finally, for $p = 1/2$ where, as previously noted, the input to the loop appears as a modulation with uncorrelated but dependent I and Q ternary data streams with identical first-order statistics [see Eq. (17)], the nonlinearities of Eqs. (26) and (27) become

$$f_1\left(u, v\right) = \frac{2\sinh\left(2u\right)}{\cosh\left(2u\right) + \cosh\left(2v\right)}$$

$$f_2\left(u, v\right) = \frac{2\sinh\left(2v\right)}{\cosh\left(2u\right) + \cosh\left(2v\right)} = f_1\left(v, u\right)$$

(29)

which suggests a balanced (symmetrical nonlinearities) cross-over type of loop.

III. Tracking Performance of the MAP Estimation Loop for QPSK with Unbalanced Data

Consider the information-reduced MAP estimation loop for phase synchronization of QPSK with dependent unbalanced ternary I and Q data illustrated in Fig. 2. The analysis of the tracking performance of the loop in Fig. 2 begins by paralleling the approach taken in [4] for the MAP-motivated loop; however, there are some significant differences that arise fairly early in the development and inhibit completion of the analysis. First, the I and Q nonlinearities in each arm of the loop in [4], namely, hyperbolic tangent functions, are not cross-coupled, i.e., each depends only on the amplified matched filter output of its respective arm. Second, several of the steps in the analysis approach carried out in [4] depend upon the I and Q nonlinearities being an odd function of their argument, which is clearly not the situation here. Finally, the assumption of independent I and Q data sequences, as was the case in [4] where the input to the loop is truly the received QPSK signal, is another important difference between the analyses when carrying the statistical averages over these sequences needed to arrive at the parameters that characterize the loop's performance. Despite these differences, we begin the analysis here in the same fashion as in [4] and proceed as far as one can go until the point is reached where certain simplifying assumptions must then be invoked.

Assuming unit input I and Q phase detector (multiplier) gains and demodulation reference signals $r_c\left(t\right) = \sqrt{2}\cos\left(\omega_c t + \hat{\theta}\right)$ and $r_s\left(t\right) = \sqrt{2}\sin\left(\omega_c t + \hat{\theta}\right)$, then, after amplification by $\sqrt{S/2}/N_0$, the sample-and-hold outputs $u_k\left(\phi\right)$ and $v_k\left(\phi\right)$ in the interval $\left(k + 1\right)T \leq t \leq \left(k + 2\right)T$ are given by

$$u_k(\phi) \triangleq \frac{\sqrt{S/2}}{N_0}\int_{kT}^{(k+1)T} y(t)r_s(t)dt = \frac{\sqrt{S/2}}{N_0}\left[T\sqrt{\frac{S}{2}}\left(E_{dk}\cos\phi - E_{uk}\sin\phi\right) - N_1\sin\phi - N_2\cos\phi\right]$$

$$v_k(\phi) \triangleq \frac{\sqrt{S/2}}{N_0}\int_{kT}^{(k+1)T} y(t)r_c(t)dt = \frac{\sqrt{S/2}}{N_0}\left[T\sqrt{\frac{S}{2}}\left(E_{dk}\sin\phi + E_{uk}\cos\phi\right) - N_2\sin\phi + N_1\cos\phi\right]$$

(30)

where N_1, N_2 are zero mean, independent Gaussian random variables[5] with variance $\sigma_{N_1}^2 = \sigma_{N_2}^2 = N_0 T \triangleq \sigma^2$ and $\phi \triangleq \theta - \hat{\theta}$ is the loop phase error. Rewriting Eq. (30) in normalized form, we have

$$u_k(\phi) = \frac{1}{2}\left[R_d\left(E_{dk}\cos\phi - E_{uk}\sin\phi\right) - \sqrt{2R_d}X_1\sin\phi - \sqrt{2R_d}X_2\cos\phi\right]$$

$$v_k(\phi) = \frac{1}{2}\left[R_d\left(E_{dk}\sin\phi + E_{uk}\cos\phi\right) - \sqrt{2R_d}X_2\sin\phi + \sqrt{2R_d}X_1\cos\phi\right]$$

(31)

where $X_i \triangleq N_i/\sigma, i = 1,2$ are normalized (unit variance) i.i.d. Gaussian random variables (RVs). Multiplying $v_k(\phi)$ by the nonlinearly processed $u_k(\phi), v_k(\phi)$ pair gives one component of the dynamic error signal, namely,

$$z_{k1}(\phi) = v_k(\phi)f_1\big(u_k(\phi), v_k(\phi)\big)$$

(32)

Similarly, multiplying $u_k(\phi)$ by the nonlinearly processed $u_k(\phi), v_k(\phi)$ pair gives the other component of the dynamic error signal, namely,

$$z_{k2}(\phi) = u_k(\phi)f_2\big(u_k(\phi), v_k(\phi)\big)$$

(33)

Finally, the total dynamic error signal, $e_k(\phi)$, in the kth signal interval is the difference of $z_{k1}(\phi)$ and $z_{k2}(\phi)$, i.e., $e_k(\phi) = z_{k1}(\phi) - z_{k2}(\phi)$.

The tracking performance of a loop such as that in Fig. 2 can, in its linear region of operation (small phase error), be characterized by the variance of the phase error which can be evaluated from the slope of the equivalent S-curve at $\phi = 0$ and the power spectral density (PSD) of the equivalent additive noise. These parameters in turn can be determined by evaluating the statistics of the signal and noise components of $z_o(t; \phi)$, making the usual assumption that the loop bandwidth is much less than the data bandwidth. With this in mind, the loop S-curve is defined as the expected value of the error signal and is given by

$$\eta(\phi) \triangleq \overline{e_k(\phi)}^{E_{dk}, E_{uk}, X_1, X_2} = \overline{v_k(\phi)f_1\big(u_k(\phi), v_k(\phi)\big) - u_k(\phi)f_2\big(u_k(\phi), v_k(\phi)\big)}^{E_{dk}, E_{uk}, X_1, X_2}$$

(34)

where the overbar denotes statistical averaging over the probability distributions of the data and noise RVs indicated, keeping in mind that the average over the data RVs must be performed jointly in accordance with Eq. (18). While, in principle, the averaging required in Eq. (34) cannot be obtained in closed form, using the properties of the nonlinearities obtained from Eqs. (26) and (27), namely that

$$f_1(u, v) = f_1(u, -v)$$

$$f_2(u, v) = -f_2(u, -v)$$

(35)

it is nevertheless possible to show analytically that the S-curve is an odd function through the origin, i.e., $\eta(\phi) = -\eta(-\phi)$, as is desirable of such a tracking characteristic. Figures 3(a) through 3(c) are

---

[5] Note that multiplication of a Gaussian process by a binary (± 1) waveform of rate $1/T$ does not change the Gaussian properties of the original process within any T-second time interval. Thus, for any input bit, the corresponding sample-and-hold outputs of the integrate-and-dump (I&D) filters are still Gaussian random variables.
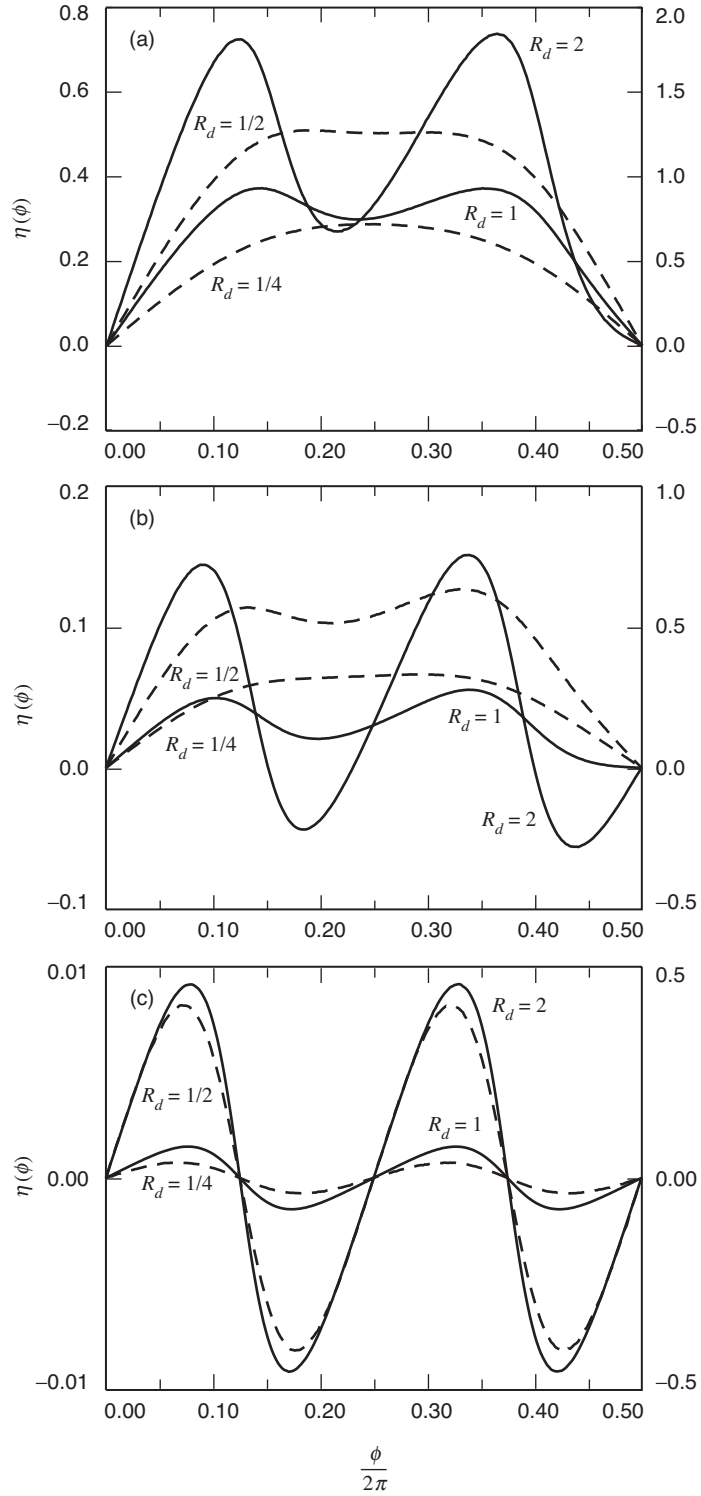
Fig. 3. Loop S-curve versus symbol SNR: (a) $p = 0.1$, **(b)** $p = 0.3$, **and (c)** $p = 0.5$. **Dashed curves correspond to the y-axis on the left, and solid curves correspond to the y-axis on the right.**

illustrations of the transitional behavior of the S-curves for $\phi \geq 0$ (obtained by computer evaluation of the averages required in Eq. (34) using MATLAB$^{\text{TM}}$ software) for three different values of p with symbol SNR R_d as a parameter. The y-axis scale on the left applies to the curves corresponding to the lower values of SNR (the dashed curves), whereas the y-axis scale on the right applies to the curves corresponding to the higher values of SNR (the solid curves). In addition, we remind the reader that in the limit of $p \to 0$ the loop becomes a PLL, and thus the S-curve has the form of $\sin \phi$.

The slope K_η of this S-curve at the origin is obtained from

$$K_\eta = \frac{d\eta(\phi)}{d\phi}\,|_{\phi=0} = \overline{u_k(0)f_1\big(u_k(0),v_k(0)\big) + v_k(0)f_1'\big(u_k(\phi),v_k(\phi)\big)\,|_{\phi=0}}^{E_{dk},E_{uk},X_1,X_2}$$

$$+ \overline{v_k(0)f_2\big(u_k(0),v_k(0)\big) - u_k(0)f_2'\big(u_k(\phi),v_k(\phi)\big)\,|_{\phi=0}}^{E_{dk},E_{uk},X_1,X_2} \qquad (36)$$

where from Eq. (31) we have made use of the relations

$$\frac{du_k(\phi)}{d\phi} = -v_k(\phi)$$

$$\qquad (37)$$

$$\frac{dv_k(\phi)}{d\phi} = u_k(\phi)$$

Also, the derivatives of the nonlinearities as denoted by the primes in Eq. (36) are given by

$$f_i'\left(u_k(\phi),v_k(\phi)\right) = \frac{\partial f_i\big(u_k(\phi),v_k(\phi)\big)}{\partial u_k(\phi)} \frac{du_k(\phi)}{d\phi} + \frac{\partial f_i\big(u_k(\phi),v_k(\phi)\big)}{\partial v_k(\phi)} \frac{dv_k(\phi)}{d\phi}$$

$$= -v_k(\phi)\frac{\partial f_i\big(u_k(\phi),v_k(\phi)\big)}{\partial u_k(\phi)} + u_k(\phi)\frac{\partial f_i\big(u_k(\phi),v_k(\phi)\big)}{\partial v_k(\phi)}, \quad i = 1,2 \qquad (38)$$

From Eqs. (26) and (27), the partial derivatives needed in Eq. (38) are given by

$$g(u,v) \triangleq \frac{\partial f_1(u,v)}{\partial u} = \frac{\partial f_2(u,v)}{\partial v}$$

$$= \frac{8p(1-p)\left\{2p(1-p) + \cosh(2v)\left[(1-p)^2\exp(2u) + p^2\exp(-2u)\right]\right\}}{\left[(1-p)^2\exp(2u) + p^2\exp(-2u) + 2p(1-p)\cosh(2v)\right]^2}$$

$$\qquad (39)$$

$$h(u,v) \triangleq \frac{\partial f_1(u,v)}{\partial v} = \frac{\partial f_2(u,v)}{\partial u}$$

$$= -\frac{8p(1-p)\sinh(2v)\left[(1-p)^2\exp(2u) - p^2\exp(-2u)\right]}{\left[(1-p)^2\exp(2u) + p^2\exp(-2u) + 2p(1-p)\cosh(2v)\right]^2}$$

13

which for $p = 1/2$ simplify to

$$g\left(u,v\right) \triangleq \frac{\partial f_1\left(u,v\right)}{\partial u} = \frac{\partial f_2\left(u,v\right)}{\partial v} = \frac{4\left[1 + \cosh\left(2v\right)\cosh\left(2u\right)\right]}{\left[\cosh\left(2u\right) + \cosh\left(2v\right)\right]^2}$$

$$h\left(u,v\right) \triangleq \frac{\partial f_1\left(u,v\right)}{\partial v} = \frac{\partial f_2\left(u,v\right)}{\partial u} = -\frac{4\sinh\left(2v\right)\sinh\left(2u\right)}{\left[\cosh\left(2u\right) + \cosh\left(2v\right)\right]^2}$$

(40)

and also could be determined directly by differentiation of Eq. (29). Finally, substituting Eq. (38) combined with Eq. (39) into Eq. (36), the slope of the S-curve becomes

$$K_\eta = \overline{u_k\left(0\right)f_1\left(u_k\left(0\right),v_k\left(0\right)\right) + v_k\left(0\right)f_2\left(u_k\left(0\right),v_k\left(0\right)\right)}^{E_{dk},E_{uk},X_1,X_2}$$

$$- \overline{\left[u_k^2\left(0\right) + v_k^2\left(0\right)\right]g\left(u_k\left(0\right),v_k\left(0\right)\right)}^{E_{dk},E_{uk},X_1,X_2}$$

$$+ \overline{2u_k\left(0\right)v_k\left(0\right)h\left(u_k\left(0\right),v_k\left(0\right)\right)}^{E_{dk},E_{uk},X_1,X_2}$$

(41)

where, from Eq. (31),

$$u_k(0) = \frac{1}{2}\left(R_d E_{dk} - \sqrt{2R_d}X_2\right)$$

$$v_k\left(0\right) = \frac{1}{2}\left(R_d E_{uk} + \sqrt{2R_d}X_1\right)$$

(42)

We note that, in an actual implementation, p would itself depend on the loop phase error (since the data decisions being fed back to the input of the loop depend on the phase of the in-phase carrier demodulation reference derived from the loop). However, since the slope of the S-curve is evaluated at $\phi = 0$, then the value of p needed in Eq. (41) is the value at $\phi = 0$, i.e., the ideal performance of the data detector. Thus, the dependence of p on ϕ is irrelevant to the evaluation of the S-curve slope.

The noise component of $e_k(t;\phi)$ (evaluated at $\phi = 0$) is given by $N_e(t) = e_k(t;0) - \eta(0) = e_k(t;0)$, which from Eqs. (32) and (33) becomes

$$N_e(t) = v_k(0)f_1\left(u_k\left(0\right),v_k\left(0\right)\right) - u_k\left(0\right)f_2\left(u_k\left(0\right),v_k\left(0\right)\right)$$

(43)

with variance

$$\sigma_{N_e}^2 = \overline{\left[v_k\left(0\right)f_1\left(u_k\left(0\right),v_k\left(0\right)\right) - u_k\left(0\right)f_2\left(u_k\left(0\right),v_k\left(0\right)\right)\right]^2}^{E_{dk},E_{uk},X_1,X_2}$$

(44)

Here again the value of p needed in Eq. (44) is the value at $\phi = 0$, which is consistent with the previous usage of the same parameter for the S-curve slope in Eq. (41).

Because of the sample-and-hold circuits shown in Fig. 2, the noise process of Eq. (43) is piecewise constant over intervals of T-second duration. Thus, as long as the loop bandwidth is much less than the

14

data bandwidth, this process can be approximated, as has been done in the past, by a delta-correlated process with correlation function given by

$$R_{N_e}(\tau) \triangleq \overline{N_e(t)N_e(t+\tau)} = \begin{cases} \sigma_{N_e}^2 \left[1 - \dfrac{|\tau|}{T} \right], & |\tau| \leq T \\[2mm] 0, & |\tau| > T \end{cases} \tag{45}$$

and equivalent single-sided noise spectral density (in the neighborhood of $f = 0$)

$$N_0' \triangleq 2 \int_{-\infty}^{\infty} R_{N_e}(\tau)d\tau = 2\sigma_{N_e}^2 T \tag{46}$$

Finally, then, the linearized phase error variance is given by

$$\sigma_\phi^2 = \frac{N_0' B_L}{K_\eta^2} \triangleq (\rho S_L)^{-1} \tag{47}$$

where $\rho = S/N_0 B_L$ is the linear loop (PLL) signal-to-noise ratio (B_L is the single-sided loop bandwidth) and, analogous to conventional quadriphase Costas loop terminology, S_L is the "quadrupling loss," which reflects the penalty paid due to the signal and noise cross-products present in $e_k(t; \phi)$. Solving for S_L from Eq. (47) gives

$$S_L = \frac{K_\eta^2}{R_d \left(N_0'/T \right)} \tag{48}$$

which unfortunately cannot be obtained in closed form for arbitrary values of p. In the limiting case of $p = 0$, however, $K_\eta = 2R_d$ and $N_0' = 4R_d T$, and thus $S_L = 1$, which corresponds to no quadrupling loss, as one would expect of a PLL.

IV. Asymptotic Behavior at Low SNR

It is of interest to examine the behavior of the information-reduced carrier synchronization scheme at low SNR (small symbol energy-to-noise ratio) since this is the region where the quadrupling loss associated with conventional carrier synchronization schemes is large and thus limits their performances. Since the outputs of the I&D filters in Fig. 2 are proportional to R_d, then for small values of this parameter, the I and Q nonlinearities can be approximated by the first few terms of their Taylor series expansion. In particular, for the $p = 1/2$ case, making the approximations $\sinh x \cong x + x^3/6$, $\cosh x \cong 1 + x^2/2$ in Eq. (29), we obtain (keeping only terms up to order x^3)

$$f_1(u, v) \cong 2 \left(u - \frac{1}{3}u^3 - uv^2 \right)$$

$$f_2(u, v) \cong 2 \left(v - \frac{1}{3}v^3 - vu^2 \right) \tag{49}$$

which when substituted in Eq. (34) results in the S-curve

$$\eta\left(\phi\right) = \frac{4}{3} \overline{\left[v_k\left(\phi\right)u_k^3\left(\phi\right) - u_k\left(\phi\right)v_k^3\left(\phi\right)\right]}^{E_{dk},E_{uk},X_1,X_2} = \frac{4}{3} \overline{u_k\left(\phi\right)v_k\left(\phi\right)\left[u_k^2\left(\phi\right) - v_k^2\left(\phi\right)\right]}^{E_{dk},E_{uk},X_1,X_2} \tag{50}$$

It is interesting (although not surprising) that the functional form of the error signal in Eq. (50) is identical to that in a conventional QPSK Costas loop (derived from MAP phase estimate considerations at low SNR) [4]. Substituting Eq. (31) into Eq. (50) and carrying out the required statistical averages results in

$$\eta\left(\phi\right) = \frac{1}{3} R_d^4 \sin 4\phi \tag{51}$$

with slope at the origin

$$K_\eta = \frac{4}{3} R_d^4 \tag{52}$$

To evaluate the equivalent noise power spectral density in Eq. (46), we need to evaluate the variance in Eq. (44), which, using the approximate expressions for the nonlinearities in Eq. (49), becomes

$$\sigma_{N_e}^2 = \frac{16}{9} \overline{u_k^2\left(0\right)v_k^2\left(0\right)\left[u_k^2\left(0\right) - v_k^2\left(0\right)\right]^2}^{E_{dk},E_{uk},X_1,X_2}$$

$$= \frac{16}{9}\left[\overline{u_k^6\left(0\right)v_k^2\left(0\right)}^{E_{dk},E_{uk},X_1,X_2} + \overline{v_k^6\left(0\right)u_k^2\left(0\right)}^{E_{dk},E_{uk},X_1,X_2} - 2\overline{v_k^4\left(0\right)u_k^4\left(0\right)}^{E_{dk},E_{uk},X_1,X_2}\right] \tag{53}$$

However, from the definitions of $u_k\left(0\right)$ and $v_k\left(0\right)$ in Eq. (31), these variables are noise-wise independent. Thus, the following first-order moments are useful in evaluating the joint moments required in Eq. (53):

$$\overline{u_k^2\left(0\right)}^{X_2} = \frac{1}{4}\left[R_d^2 E_{dk}^2 + 2R_d\right]$$

$$\overline{v_k^2\left(0\right)}^{X_1} = \frac{1}{4}\left[R_d^2 E_{uk}^2 + 2R_d\right]$$

$$\overline{u_k^4\left(0\right)}^{X_2} = \frac{1}{16}\left[R_d^4 E_{dk}^4 + 12R_d^3 E_{dk}^2 + 12R_d^2\right]$$

$$\overline{v_k^4\left(0\right)}^{X_1} = \frac{1}{16}\left[R_d^4 E_{uk}^4 + 12R_d^3 E_{uk}^2 + 12R_d^2\right] \tag{54}$$

$$\overline{u_k^6\left(0\right)}^{X_2} = \frac{1}{64}\left[R_d^6 E_{dk}^6 + 30R_d^5 E_{dk}^4 + 180R_d^4 E_{dk}^2 + 120R_d^3\right]$$

$$\overline{v_k^6\left(0\right)}^{X_1} = \frac{1}{64}\left[R_d^6 E_{uk}^6 + 30R_d^5 E_{uk}^4 + 180R_d^4 E_{uk}^2 + 120R_d^3\right]$$

Using Eq. (54), the joint averages over the data sequences of the terms in Eq. (53) become

$$\overline{u_k^6(0)\,v_k^2(0)}^{E_{dk},E_{uk},X_1,X_2} = \overline{v_k^6(0)\,u_k^2(0)}^{E_{dk},E_{uk},X_1,X_2}$$

$$= \frac{1}{16}\left(4R_d^7 + 30R_d^7 + 60R_d^5 + 15R_d^4\right) \tag{55}$$

$$\overline{v_k^4(0)\,u_k^4(0)}^{E_{dk},E_{uk},X_1,X_2} = \frac{1}{16}\left(12R_d^6 + 36R_d^5 + 9R_d^4\right)$$

which upon substitution in Eq. (53) gives

$$\sigma_{N_e}^2 = \frac{1}{9}\left(8R_d^7 + 36R_d^6 + 48R_d^5 + 12R_d^4\right) \tag{56}$$

Finally, using Eq. (56) in Eq. (46) together with Eq. (52), the quadrupling loss as computed from Eq. (48) becomes

$$S_L = \frac{1}{1 + \dfrac{9}{2R_d} + \dfrac{6}{R_d^2} + \dfrac{3}{2R_d^3}} \tag{57}$$

which is identical to the result for the conventional QPSK Costas loop derived from MAP carrier phase estimation considerations at low SNR [4, Eq. (35)]. What is particularly interesting about this result is that, despite the fact that for $p = 1/2$ the effective I and Q sequences that are input to the iterative information-reduced loop are ternary in nature and not independent of each other, whereas in the conventional QPSK Costas loop they are i.i.d. binary and independent, the quadrupling loss is nevertheless the same in the limit of low SNR operation of the former.

Thus, we see that at the outset of the iteration process, the information-reduced QPSK loop performs the same as the conventional QPSK loop. However, as the loop continues to produce better and better carrier phase estimates, p continues to decrease, and thus the quadrupling loss performance of the loop varies between its value as given by Eq. (57) and its value corresponding to the error rate performance of the data detector at the particular value of R_d under consideration. (In the limit of $p \to 0$, the quadrupling loss would disappear entirely.) By contrast, the quadrupling loss of the conventional QPSK loop remains fixed at its value as determined from Eq. (57). In the following section, we will demonstrate this more quantitatively with numerical results obtained by computer simulation.

V. Evaluation of the Tracking Performance as a Function of Detection SNR

As discussed in the previous section, the amount of quadrupling loss is commonly used as a measure of the tracking performance degradation of QPSK carrier synchronization loops. With this in mind, Fig. 4 is a plot of the quadrupling loss S_L of the information-reduced QPSK loop versus detection (symbol) SNR R_d with p as a parameter. These results were obtained by computer simulation (MATLAB$^{\text{TM}}$ numerical methods) of the statistical averages required to compute the S-curve slope K_η and equivalent noise PSD N_0' needed in Eq. (48). While we recognize that, even for perfect carrier synchronization, any given form of coded modulation and associated data detector/decoder results in a value of p that is a function of R_d, we have chosen to maintain p as a constant parameter in this figure. The reason for this is that the results presented there can then be independent of the specific form of data detector or, equivalently, the specific form of error correction coding employed, provided that the conditions for an i.i.d. and noise-dependent error sequence are still met. For any given coding application, only a single point on each curve of constant p would be applicable, namely, the one corresponding to the given error
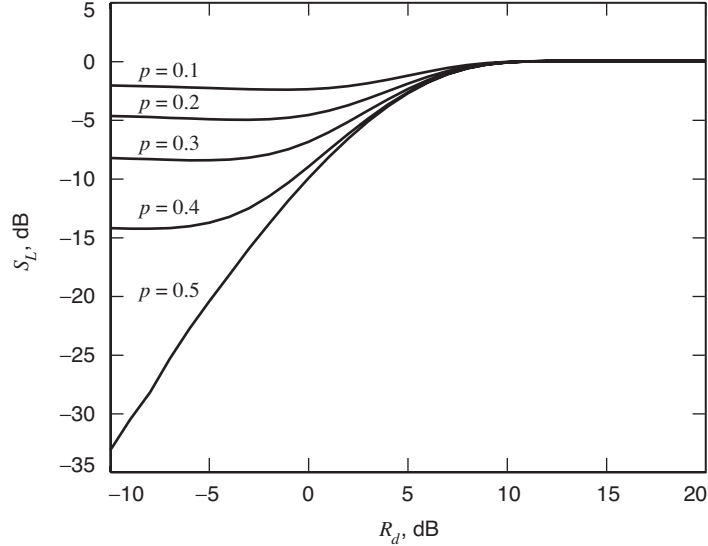
Fig. 4. Quadrupling loss versus symbol SNR in decibels with p as a parameter.

rate behavior of the data detector (decoder), and thus the performance for that particular application would be illustrated by a single curve passing through this series of points.

We observe from the results in Fig. 4 the monotonic behavior of the quadrupling loss as a function of p.[6] Although somewhat cumbersome to evaluate analytically, the limiting behavior of this loss at low SNR is given by

$$\lim_{R_d \to 0} S_L = (1 - 2p)^2 \tag{58}$$

which is the identical result obtained for the information-reduced BPSK loop in [1]. Furthermore, we observe the immediate large improvement in quadrupling loss at low SNR as soon as some degree of fidelity of the data decisions begins to take place. More specifically, for improvement to take place in the carrier synchronizer, the data estimator is not required to operate with symbol-error probabilities as small as those typically needed for reliable communication. In fact, when used in the manner illustrated in Fig. 1, a value of $p = 0.1$, which in most applications would be considered unacceptable for data decisions, can result in dramatic improvement in carrier synchronization performance relative to that of the conventional QPSK Costas loop as represented by the curve labeled $p = 0.5$. It should be further noted that, although this curve was obtained by computer simulation, it agrees with the theoretical result in Eq. (57).

Another interpretation of the numerical results can be obtained by recognizing that the loop SNR $\rho = S/N_0 B_L$ can be expressed in terms of the symbol SNR $R_d = ST/N_0$ by $\rho = R_d/B_L T$, which when substituted in Eq. (47) gives an expression for the normalized phase error variance as

$$\frac{\sigma_\phi^2}{B_L T} = (R_d S_L)^{-1} \tag{59}$$

Figure 5 is a plot of this normalized variance, with S_L determined as in Fig. 4 versus R_d with p as a parameter. As one would anticipate, here the curves are both monotonic with p for fixed R_d and

---

[6] At the same time, we note that for fixed p we cannot guarantee a monotonic performance with SNR.
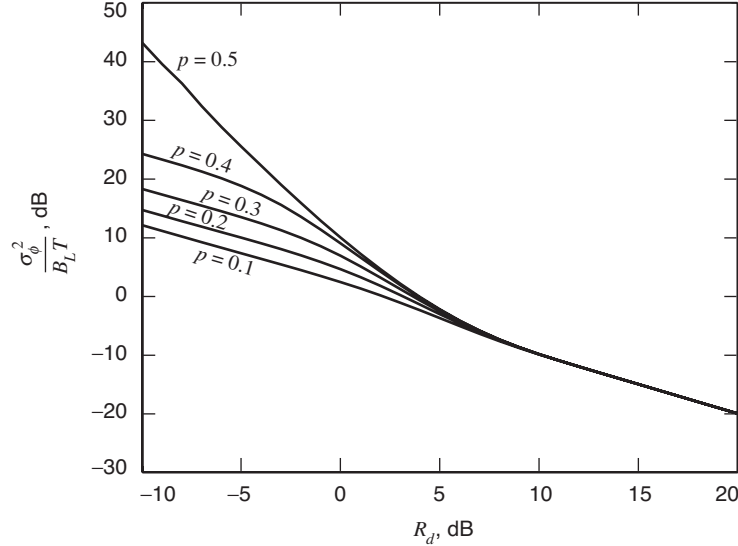
**Fig. 5. Normalized phase error variance versus symbol
SNR in decibels with p as a parameter.**

monotonic with R_d for fixed p. These curves represent the tracking performance of the loop when the loop bandwidth–symbol time product is held fixed and once again show the rapid dramatic improvement with data detection efficiency at low SNR for the information-reduced QPSK loop. Here again we see the dramatic improvement in performance at low SNR as the information reduction increases, i.e., the data estimates improve.

VI. Sensitivity to Mismatch

Having improved the phase tracking by the use of data feedback, the new improved carrier phase estimate will help the data detector obtain better symbol estimates, which suggests an iterative procedure. That is, the phase tracking loop is initially designed assuming a value of p corresponding to no feedback. The initial data estimates obtained using this particular structure as a carrier synchronizer are fed back, and the carrier synchronizer structure then is modified based on the new estimated value of p. This updated carrier synchronizer provides improved phase tracking, which in turn provides improved data detection. These new data estimates, having a smaller value of p, then are fed back to the input of the carrier synchronizer and the iteration continues. Thus, in practice, at any given time instant there will be a mismatch between the true value of p associated with the input error sequence and its estimate, $\hat{p}$, used to implement the nonlinearities of Eqs. (26) and (27) in the loop. As such, we wish to investigate the sensitivity of the loop performance as measured by the quadrupling loss to mismatch between p and $\hat{p}$. That is, how good must our estimate of p be for the purpose of loop implementation and yet still achieve an improvement in performance relative to not implementing decision feedback at all?

We begin this discussion by recognizing that when p and $\hat{p}$ are unequal, the quadrupling loss expression of Eq. (48) is still appropriate provided that, in the expressions used to compute K_η and N_0', $\hat{p}$ is substituted for p in the definitions of the nonlinearities in Eqs. (26) and (27) as well as their derivatives in Eq. (39). The first point to observe is that, for $\hat{p} = 0.5$, $f_1(u,v)$ and $f_2(u,v)$ and their associated derivatives simplify to the forms in Eqs. (29) and (40), respectively, which in view of the symmetry properties of these functions results in the averages over the data sequences E_{uk} and E_{dk} needed to evaluate K_η and N_0' becoming independent of p. This in turn results in the quadrupling loss also becoming independent of p. That is, if we assume $\hat{p} = 0.5$ for the loop design, then the performance is independent of the true data input probabilities. Next, suppose that we are optimistic in our estimate of p used for the design of the loop, i.e., $\hat{p} \leq p$. Figures 6(a) and 6(b) are plots of the squaring loss as determined
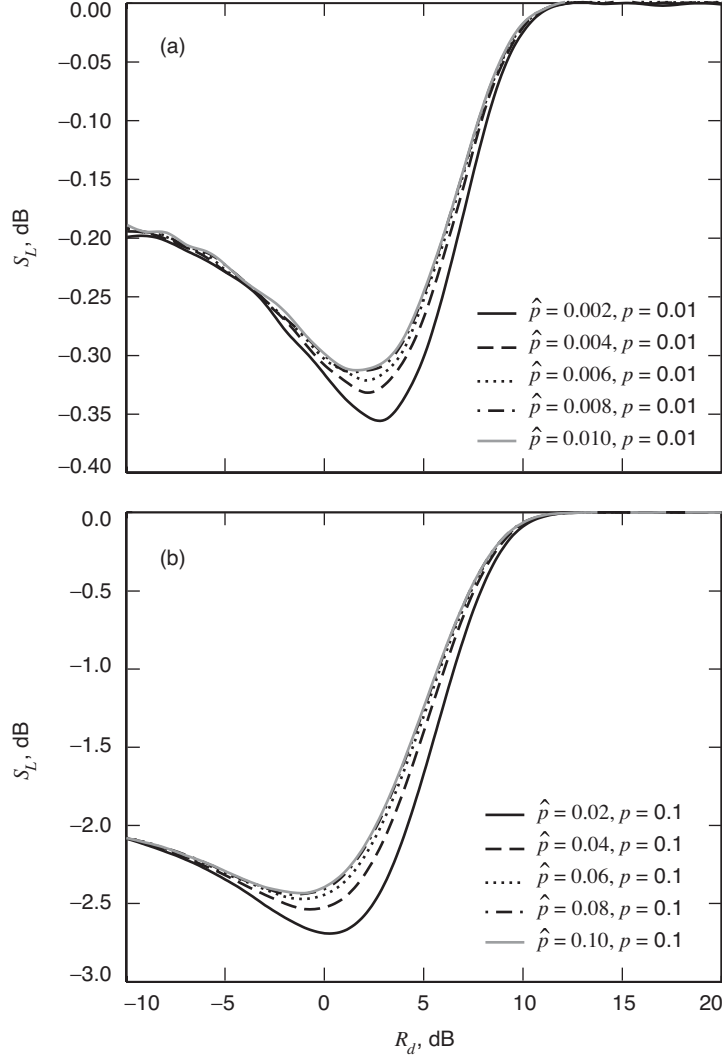
19

Fig. 6. Quadrupling loss performance in the presence of mismatch: (a) $p = 0.01, \hat{p} \leq p$ **and (b)** $p = 0.1, \hat{p} \leq p$.

from Eq. (48) versus R_d in decibels with $\hat{p}$ as a parameter and $p = 0.01$ and $p = 0.1$, respectively. The deviation between p and $\hat{p}$ is as much as a factor of 5. We see that for this case the performance of the loop is quite insensitive (a variation on the order of 0.1 dB or less) to the mismatch and yet we still obtain a significant improvement relative to the case of no feedback at all. Figures 7(a) and 7(b) show the analogous results for the case where we are pessimistic in our estimate of p used for the design of the loop, i.e., $\hat{p} \geq p$. Although we see a bit more sensitivity of the loop performance to the mismatch between p and $\hat{p}$, in all cases performance is as good or better than the case of no feedback (information reduction) at all. It is also interesting to note in these figures that, except for the singular case of $\hat{p} = 0.5$, the limiting quadrupling performance as $R_d \rightarrow 0$ behaves like $(1 - 2p)^2$ independently of the amount of mismatch and thus is consistent with Eq. (58) for the perfectly matched case. For $\hat{p} = 0.5$, as previously mentioned, the performance is independent of the true value of p and becomes synonymous with that of the conventional Costas loop.
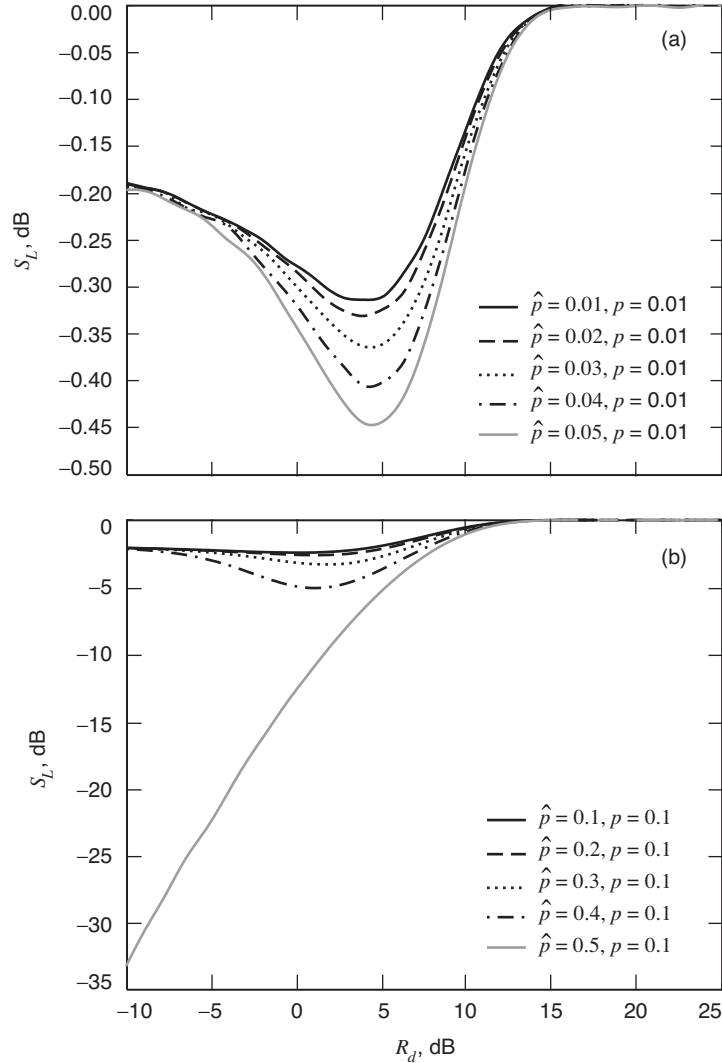
Fig. 7. Quadrupling loss performance in the presence of mismatch: (a) $p = 0.01, \hat{p} \geq p$ **and (b)** $p = 0.1, \hat{p} \geq p$.

VII. Conclusions

Using the same iterative information-reduction principle previously introduced for carrier synchronization of coded BPSK, it is possible to design an analogous closed-loop configuration for coded QPSK that outperforms the conventional I-Q schemes. It has been shown that very accurate symbol decisions are not required in order to achieve significant improvements in low SNR tracking threshold (or, equivalently, operation with greatly reduced phase error) as measured by the reduction in the quadrupling loss of the loop. Stated another way, the new QPSK carrier synchronization loop can operate effectively at signal levels that might be too low for a conventional I-Q loop to even lock. Furthermore, once phase-locked, the loop continues to iteratively improve its performance by transferring its phase estimates to the data detector and receiving in return improved data decisions to modify its I and Q nonlinearities, all the while attempting to approach the tracking performance of a phase-locked loop operating on an unmodulated tone.

Finally, it should be noted that the same information-reduction principle can in principle be applied to offset QPSK (OQPSK) to generate a carrier tracking loop for such a modulation. However, in this case the effective ternary I and Q sequences generated at the input to the loop now occur at twice the data rate (because of the half-symbol offset between the transmitted I and Q data streams), and furthermore these effective data sequences are now themselves correlated in time in addition to being jointly dependent. Because of this, analysis of the behavior of such a loop is difficult if not impossible, and thus the performance would need to be obtained by computer simulation. Such a task is left as an exercise for the interested reader.

References

[1] M. K. Simon and V. A. Vilnrotter, "Iterative Information-Reduced Carrier Synchronization Using Decision Feedback for Low SNR Applications," *The Telecommunications and Data Acquisition Progress Report 42-130, April–June 1997*, Jet Propulsion Laboratory, Pasadena, California, pp. 1–21, August 15, 1997.
http://ipnpr/progress_report/42-130/130A.pdf

[2] V. Vilnrotter, A. Gray, and C. Lee, "Carrier Synchronization for Low Signal-to-Noise Ratio Binary Phase-Shift-Keyed Modulation Signals," *The Telecommunications and Mission Operations Progress Report 42-139, July–September 1999*, Jet Propulsion Laboratory, Pasadena, California, pp. 1–16, November 15, 1999.
http://ipnpr/progress_report/42-139/139I.pdf

[3] V. Vilnrotter, C. Lee, and N. Lay, "A Generalized Pre-Processor for Block and Convolutionally Coded Signals," *The Telecommunications and Mission Operations Progress Report 42-144, October–December 2000*, Jet Propulsion Laboratory, Pasadena, California, pp. 1–19, February 15, 2001.
http://ipnpr/progress_report/42-144/144G.pdf

[4] M. K. Simon, "On the Optimality of the MAP Estimation Loop for Carrier Phase Tracking BPSK and QPSK Signals," *IEEE Transactions on Communications*, vol. COM-27, no. 1,, pp. 158–165, January 1979.